Nepal earthquake evidence from GNSS data at the Everest Pyramid Lab

G. PORETTI[1]*, F. MORSUT[1] & F. PETTENATI[2]

[1]*Department of Mathematics and Geosciences, University of Trieste, Italy*

[2]*Istituto Nazionale di Oceanografia e di Geofisica Sperimentale – OGS, Trieste, Italy*

**Correspondence:* *porettig2@gmail.com*

Abstract: The permanent GNSS station located at the Everest Pyramid Laboratory of EvK2CNR recorded its position coordinates during the earthquakes at the Gorkha (25 April 2015) and Ghorthali zones (12 May 2015) at an interval of every 30 s. The data recorded over three days prior to and after the earthquakes were analysed and the movement indicated a shifting of the GNSS station point from its original position every 30 s. From an accurate analysis of the coordinates of the station determined using GNSS Bernese software, it is possible to detect the movements of the station during the seismic events.

The shifts in the GNSS point were summed to provide an integral function (PIF, Pyramid Integral Function) that can be computed for each of the three components. Comparing them with the displacement record of the GURALP broadband seismic station (IO-EVN) of the OGS (Istituto Nazionale di Oceanografia e di Geofisica Sperimentale, OGS, Trieste), located at the Pyramid, it is possible to establish a correlation, particularly with the vertical and north components; the maxima of the PIF coincide with the time of occurrence of the earthquakes.

At 06:11 UTC on 25 April 2015, an earthquake of moment magnitude (M_w) 7.8 occurred with its epicentre in the Gorkha zone (Nepal), NW of Kathmandu. The sub-horizontal movement was a purely inverse slip, with low dip angle and unzipping the lower edge of the locked portion (Avouac *et al.* 2015). It was connected with the Main Himalayan Thrust (MHT; Denolle *et al.* 2015). The rupture propagated eastwards for 140 km producing a great sequence of aftershocks all located east of the main shock (Adhikari *et al.* 2015), with an aftershock of M_w 7.3 on 12 May 2015, located east of Kathmandu in the Ghorthali zone, about 60 km WSW of the Pyramid Laboratory of EvK2CNR. Since May 2014, a broad band seismometer GURALP 60 s (IO-EVN) has been operating in the Pyramid Laboratory, which recorded all the sequence of seismic events (Pettenati *et al.* 2014). The data, recorded at 20 samples per second (SPS), were used to estimate the co-seismic movement of a wide range of seismic events. The station is useful for recording many small events, which were not detected by Huang *et al.* (2016), using a match filter technique based on the data (100 SPS) of a local seismic network of 11 stations operated by the China Earthquake Network Center in Tibet.

The MHT is the unique result of the subduction of two continents, the Indian and Eurasian plates, which significantly adjusts the shortening in the Nepal area (20 mm a^{-1}) (Bilham *et al.* 1997; Ader *et al.* 2012). A detailed image of the ruptured portion of the Gorkha earthquake was presented by Galetzka *et al.* (2015) using the data (5 SPS) of a network of six GPS stations and three low-rate GPS stations. They recognized a slip pulse of the source and its interference with the Kathmandu basin. Grandin *et al.* (2015) studied the rupture process of the 2015 main shock, recognized its strong direction towards the ESE of the rupture evolution, and also connected it with the segmentation of the MHT. A review of the seismic deformation of the 2015 Gorkha earthquake was presented at the 2015 Himalaya–Karakoram–Tibet (HKT) workshop by Jouanne (2015).

A permanent GNSS station (PYRA) has been operating at the EvK2CNR Pyramid Laboratory near the Base Camp of Mount Everest since 2002 (Fig. 1a). Currently, a Leica GRX1200+GNSS receiver is installed with an AT504 LEIS antenna sampling at a rate of 30 s. From 2002 to 2009, PYRA was used as an experimental station. The recording data were not continuous because of its experimental purpose, but one could analyse some long intervals of observations (at least 24 h for some days in 2003 and 2004) using Leica LGO (Leica Geo Office) software and a double difference approach with the IGS LHAZ (Lhasa, China) station as a reference station. Despite a very long baseline (about 450 km),it was possible to estimate a movement of 4.5 cm a^{-1} with an azimuth of 25° with the help of a commercial software such as LGO (Poretti *et al.* 2010, 2011).

After 2009 the GNSS station was connected to the Internet and the data (in RINEX format) made

From: Sharma, R., Villa, I. M. & Kumar, S. (eds) *Crustal Architecture and Evolution of the Himalaya–Karakoram–Tibet Orogen*. Geological Society, London, Special Publications, **481**, 7–18.
First published online July 31, 2019, https://doi.org/10.1144/SP481-2017-71

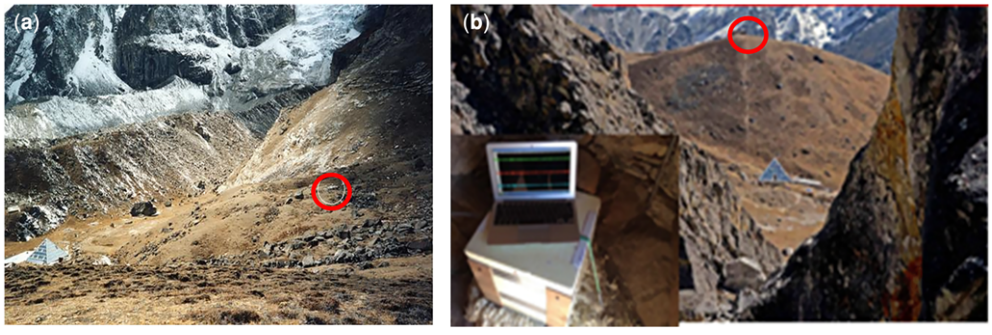

Fig. 1. The location of the GNSS (red circle) in (**a**) 2003 and (**b**) post-2009, respective to the Pyramid Laboratory (visible in the photos).

Table 1. *IGS stations used for processing the PYRA data*

Station code	Station name	Date	Latitude WGS84 (°)	Longitude WGS84 (°)	Elevation WGS84 (m)
PYRA	Pyramid	17 October 2015	27.9575380	86.8149573	5032.254
HYDE	Hyderabad	17 October 2015	17.4172616	78.5508733	441.690
KIT3	Kitab	17 October 2015	39.1347674	66.8854487	622.480
LCK3	Luknow	17 October 2015	26.9121797	80.9556362	64.168
LCK4	Luknow	17 October 2015	26.9121430	80.9556171	64.184
LHAZ	Lhasa	17 October 2015	29.6573335	91.1040305	3624.598
PBRI	Port Blair	17 October 2015	11.6377803	92.7121365	−22.491
URUM	Urumqui	17 October 2015	43.8079498	87.6006702	858.884

The 'Date' field indicates the date when the position was recorded (double difference process, 24 h of data).

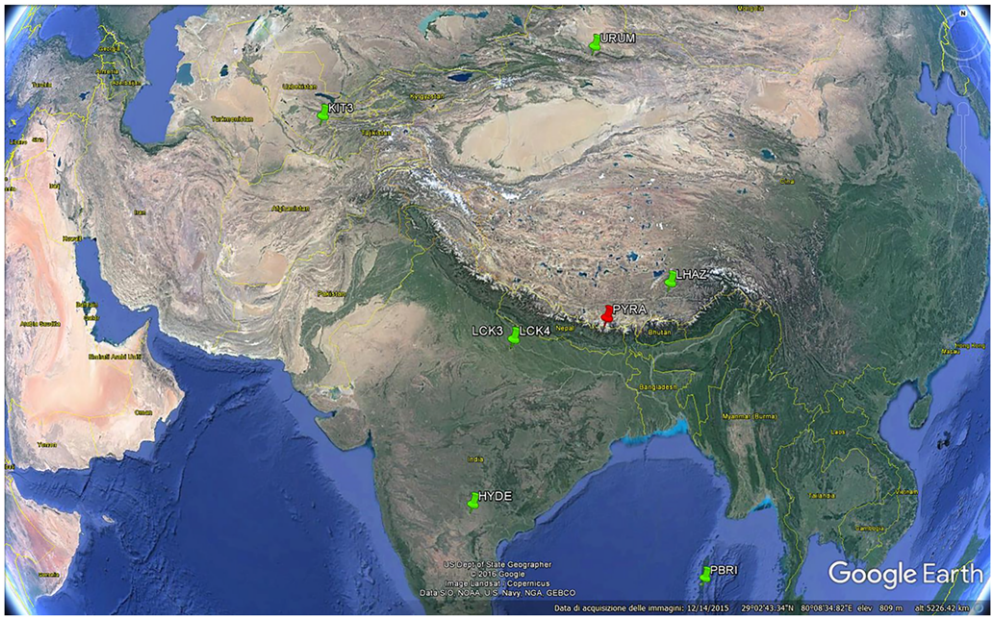

Fig. 2. Google Earth map of Central Asia with the locations of the IGS stations used in this research (green) and the Pyramid Lab (red). (Data: SIO, NOAA, US Navy, NGA, GEBCO. Image Landsat/Copernicus).

available to the scientific community through a server at the Department of Mathematics and Geosciences, University of Trieste (ftp://140.105.121.42). On this occasion, the Pyramid point was shifted to a new location that was more stable from a geological and topographical point of view (Fig. 1b). The preliminary results of this work were presented at the 2015 HKT workshop (Poretti *et al.* 2015). It is important to report that the EvK2 Pyramid station is close to the border of a high coupling zone and an area of a seismicity cluster (Avouac *et al.* 2015, fig. 1, approximately at the intersection of the 87° E meridian and the 28° N parallel). The station is located on a body of gneissic rocks in a shelter 250 m away from the Pyramid, connected by a powerline adapter 500 Mbps.

In this paper, the data recorded for a period of three days prior to, and after, the earthquakes are presented. The movements of the Pyramid station were precisely detected during the 2015 Gorkha earthquake. The study reveals that the comparison of the Pyramid Integral Functions (PIF) with the displacement record of the seismograph station is a possible way to establish a correlation, especially with the vertical and north components. The maxima of the PIF coincide with the time of occurrence of the earthquakes.

GNSS data processing

The precise coordinates of the Pyramid Laboratory GNSS Station (PYRA), were determined with reference to 7 IGS stations: Hyderabad (HYDE, India), Kitab (KIT3, Uzbekistan), Lucknow (LCK3, LCK4, India) Lhasa (LHAZ, Tibet), Port Blair (PBRI, India) and Urumqi (URUM, China). In Table 1 and Figure 2 these stations are presented with their names and coordinates (WGS84).

The sampling rate of these stations is 30 s and the RINEX files were downloaded from the UNAVCO FTP server (ftp://data-out.unavco.org/pub/rinex/). The PYRA data were downloaded from our FTP server. In order to achieve a high precision for our surveys, Bernese Scientific Software 5.2 was used with the following files for controlling and modelling the common errors:

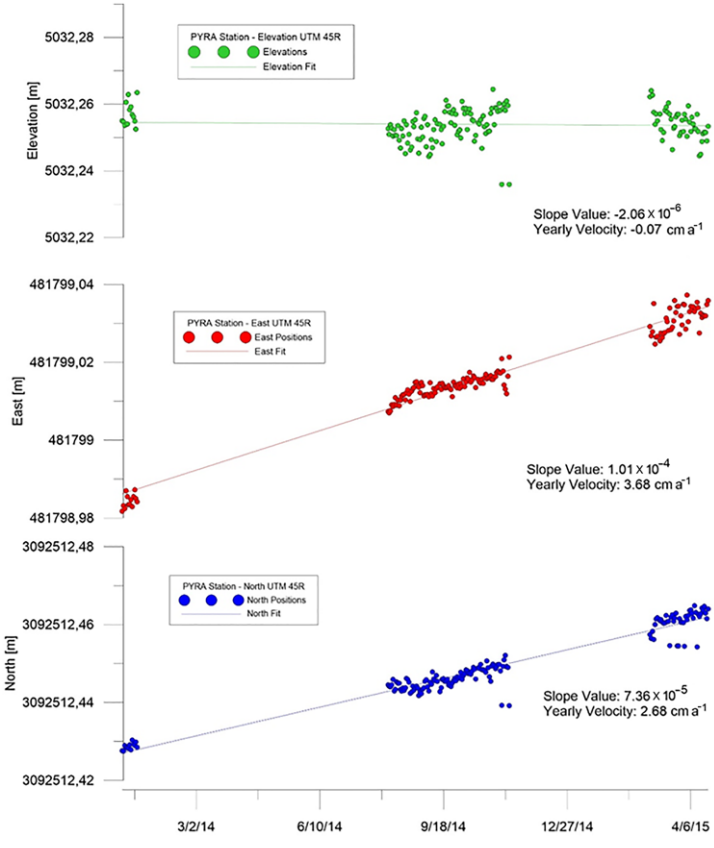

Fig. 3. PYRA station time-series analysis, slopes and velocities (1 January 2014–20 April 2015).

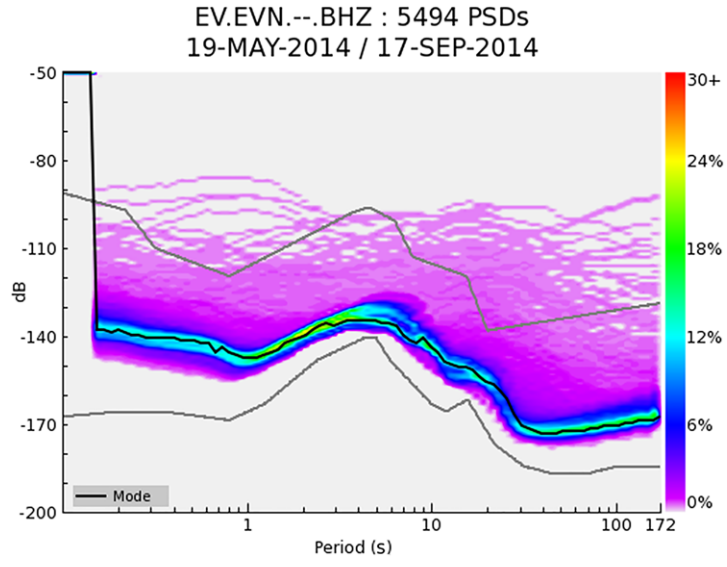

Fig. 4. Data quality of IO-EVN OGS station at Pyramid EvK2.

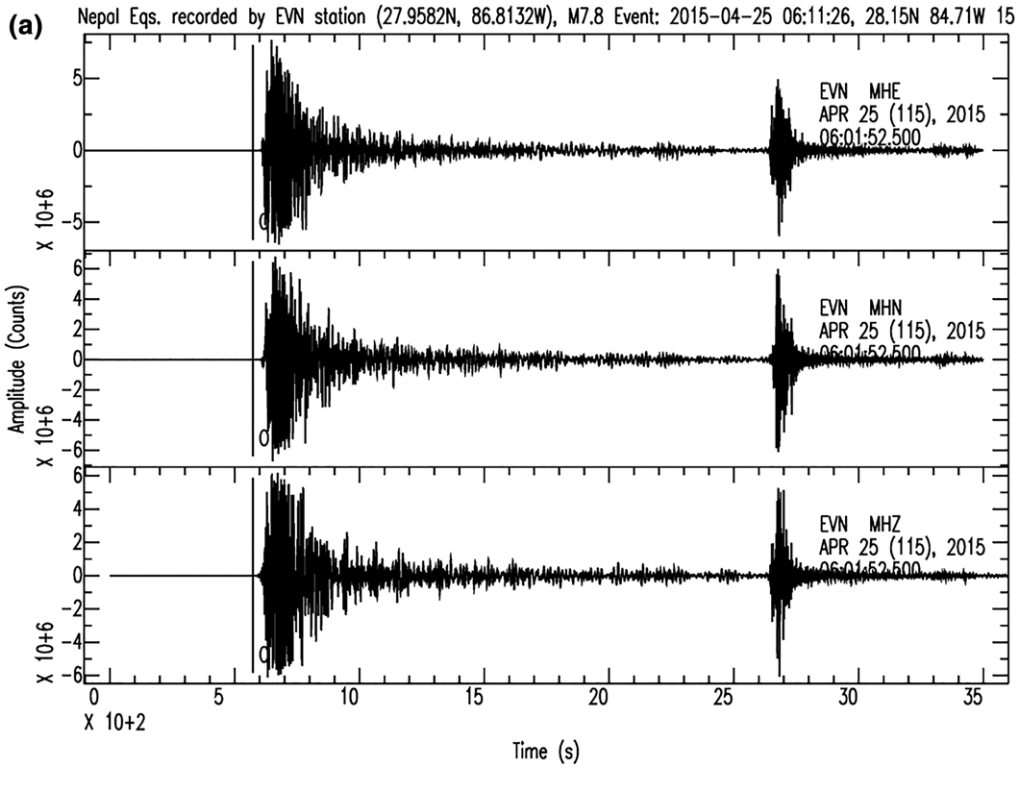

Fig. 5 (**a**) First 30 s records of the M_w 7.8 Gorkha earthquake of 25 April 2015, by the IO-EVN station of the OGS, close to the Everest Pyramid Laboratory of EvK2CNR. Top panel shows the EW component; middle panel shows the NS component; and bottom panel shows the vertical component.

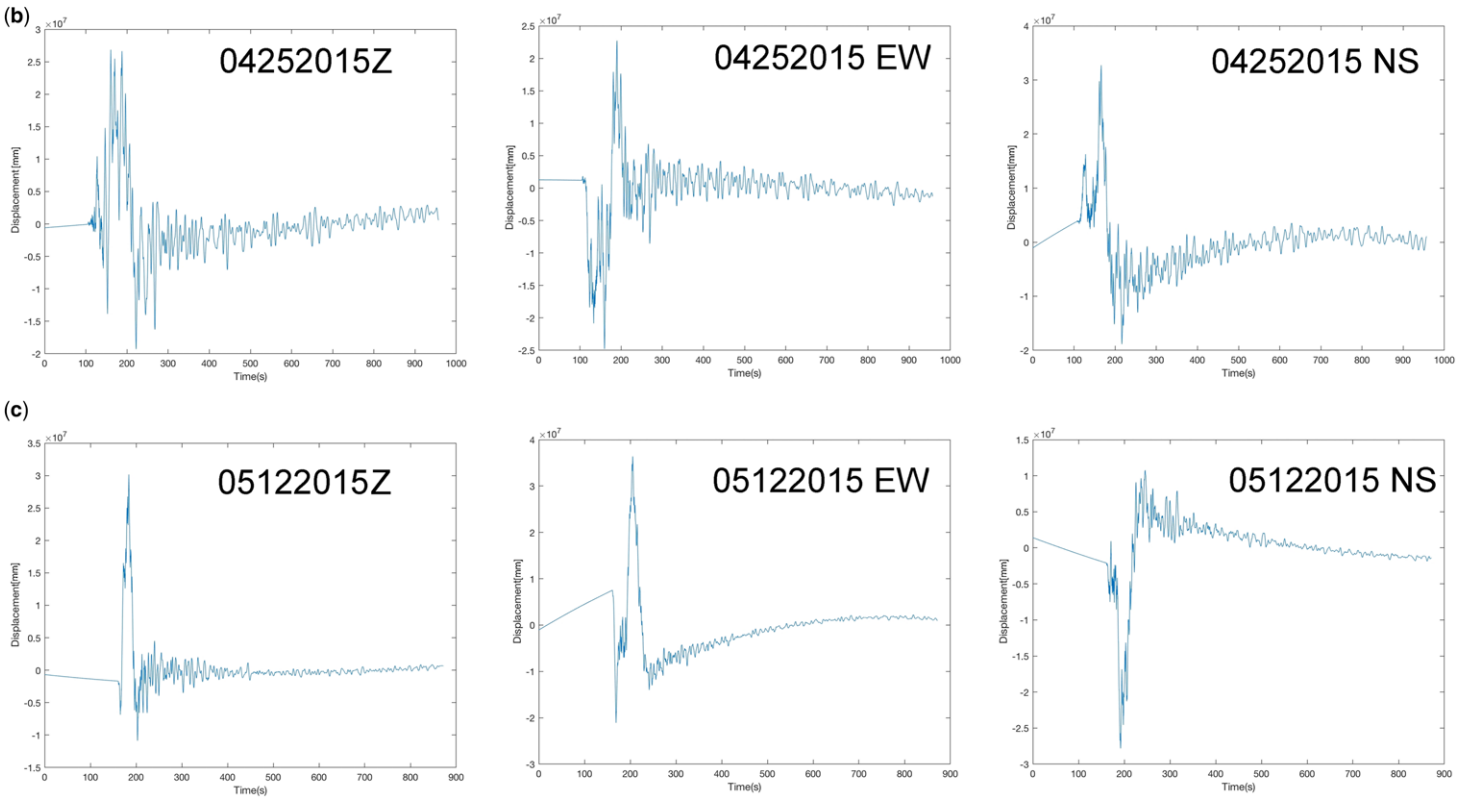

Fig. 5. *Continued*. (**b, c**) From IO-EVN Guralp broadband station close to Pyramid EvK2, displacements of the three components of (b) the Gorkha main shock of 25 April 2015 M_w 7.8 and (c) the Ghorthali shock of 12 May 2015 M_w 7.3. The origin time of the main shock is 06 10′ UTC, while the origin time of the Ghorthali M_w 7.3 is 07 05′ UTC.

- from the Center for Orbit Determination in Europe (CODE, ftp://ftp.unibe.ch) we downloaded Precise Ephemerides for satellites (EPH files – GPS and GLONASS), ionospheric error modelling (ION files), clock satellite biases (CLK files, only for GPS), Earth parameters (ERP files) and P1C1-P1P2 biases (DCB files);
- for the tropospheric model, the Vienna Mapping Function 1 was used with its 6 h grid map, for wet and dry components (VMF1 files, http://ggosatm.hg.tuwien.ac.at/DELAY/GRID/VMFG);
- to reduce ocean tidal loading error, the FE2004 model was used (BLQ file, http://holt.oso.chalmers.se/loading/);
- for atmospheric tidal loading, internal Bernese processing was used (file ATM).

All these data were downloaded using custom Python scripts and were present for every daily elaboration.

Time-series recorded before the earthquakes (2014–15)

The position of the Pyramid Laboratory GNSS Station was determined by processing the long series recorded between 2014 and 2015 (Fig. 3). For this elaboration, the BPE (Bernese Process Engine) was useful for automating a very long process, determining a starting position for every station with a Precise Point Positioning technique (PPP on 24 h data) and performing a more precise positioning using a double difference technique (DD on 24 h data) (Dach *et al.* 2007). It can be seen that the data are not continuous because of some technical problems at the Pyramid Laboratory (lack of electrical power and loss of Internet connection), but they permit calculation of a fitting line and determination of a movement velocity for each coordinate. With a movement velocity of 2.68 cm a^{-1} along the north axis and 3.68 cm a^{-1} along the east axis, the annual velocity displacement of the PYRA station is about 4.55 cm a^{-1}, confirming the previous analysis conducted in 2009 (Poretti *et al.* 2010, 2011).

The records of April and May 2015

The broadband station IO-EVN

The broadband seismometer GURALP 60s – 50 Hz, CMG-3TD with 24-bit Gurlp digitizer, was installed at the EvK2CNR Pyramid Laboratory to record data in continuous mode at 20 SPS. The connection with OGS is by satellite and soon after the main shock access to the data via the Internet was made public, as per the agreement of EvK2CNR. The principal application for a Power Spectral Density (PSD) measurement of physical data is to establish a probabilistic description for the instantaneous values of the data (Bendat & Piersol 2010). Figure 4 shows the PSD of the quality of noise with respect to the low and high noise levels of the world. Some patterns of high PSD values (−110 to −80 dB) visible for long periods are due to the data produced during the occurrence of small earthquakes. One can see that the quality and the sensitivity of the data are reasonably good. The high-quality data from this station allowed Huang *et al.* (2016) to detect about 1500 new small magnitude earthquakes, using a matched filter method (Gibbons & Ringdal 2006). These small events were not noticed by the local network.

The station recorded all the sequence, with the distribution of the aftershocks towards it (east of the main shock, Adhikari *et al.* 2015, fig. 3). As mentioned in the introduction, IO-EVN was in a strategic position because it is in the direction of maximum propagation of slip on the fault, towards the east (directivity) (Grandin *et al.* 2015). The M_w 7.3 Ghorthali event, the biggest aftershock, was transmitted in real time. Its epicentre was about 60 km from the station, whereas the main shock occurred at a distance of 160–170 km from the Pyramid. Figure 5a shows the three components of the main shock and its aftershock of M_w 6.3, illustrating that the horizontal components were not sufficiently saturated.

Figure 5b show the three components (Z, NS and EW) of the IO-EVN Guralp displacement recorded during the main shock of 25 April, while Figure 5c presents the three components of the M_w 7.3 aftershock that occurred on 12 May 2015. The integration was carried out by a previous detrend of the velocity data and a subsequent detrend of displacement data, and by a band filter 0.1–10 Hz. A comparison with PYRA data is difficult.

The first comparison of two events on the NS components suggests an opposite movement direction, towards the south for the main shock with oscillation to the north, and a net displacement to the north for the 12 May event. Both displacements seem to have no residual offset of the deformation. The other two components are similar, with a clearer vertical down-pulse of the 12 May shock.

The Gorkha earthquake (20–30 April 2015)

The positions of the different IGS stations before (20 April 2015) and after (30 April 2015) the earthquake are shown in Tables 2 and 3. The geographical coordinates WGS84 with their relative RMS are presented and the methodology used to analyse these data is the same as in the previous cases.

To analyse the displacement movement during the earthquake, an in-depth analysis was conducted using a kinematic approach on the GNSS data from 24–26 April. After the above elaborations, the PYRA stations were set as ‘kinematic stations’ while all the other stations were treated as ‘fixed stations’,

Table 2. *Station positions on 20 April 2015*

	Latitude (°)	Longitude (°)	Elevation (m)	RMS-Lat. (m)	RMS-Lon. (m)	RMS-Elev. (m)
HYDE	17.4172614	78.5508731	441.686	0.00036	0.00049	0.00145
KIT3	39.1347674	66.8854485	622.490	0.00036	0.00041	0.00148
LCK3	26.9121796	80.9556361	64.168	0.00039	0.00 -41	0.00158
LCK4	26.9121429	80.9556170	64.184	0.00039	0.00041	0.00157
LHAZ	29.6573335	91.1040304	3624.596	0.00039	0.00034	0.00153
PYRA	27.9575383	86.8149578	5032.245	0.00056	0.00060	0.00254
PBRI	11.6377802	92.7121366	−22.507	0.00068	0.00062	0.00230
URUM	43.8079498	87.6006701	858.883	0.00040	0.00036	0.00181

RMS is calculated in metres on 24 h data.

therefore making it possible to investigate if the PYRA moved compared to them every 30 s. Figure 6 presents results in the form of three graphs, one for each coordinate (UTM 45R) and the dotted line represents the earthquake at 06:11 UTC. It is possible to state that there was a horizontal movement, with a period of 'assessment', followed by a normal trend. However, with a centimetre difference in position, the elevation movement is not evident or it is lower than the measurement of noise. Using UTM coordinates, it was possible to determine the movement derived from the earthquake (in metres), from 20 to 30 April 2015 (Table 4).

Co-seismic displacements: relative movements between the PYRA and other IGS stations

The distances of these points from the Pyramid Lab are rather large but they can be calculated with reliable accuracy using Bernese Software and providing Cartesian station positions calculated as mentioned above. In order to detect an eventual shift of the points during the earthquake, the distances were computed before and after the earthquake (Table 5).

The distances present centimetre differences, compatible with the movement observed during the earthquake. Another interesting observation concerns the direction of movement: URUM and LHAZ are located to the north with respect to PYRA, on the Eurasian Plate, and the distances increased after the earthquake, indicating extension and a southward movement of PYRA (as shown in our prior analysis). KIT3 is located on the Eurasian Plate too, but at a greater distance than the other stations and is located to the west with respect to PYRA. As shown above, no westward movement was detected and a significant difference is not expected for this station. The other stations (HYDE, LCK3, LCK4, PBRI) are located on the Indian Plate and present an opposite (negative) relative movement, so their distances with respect to PYRA, decreased after the earthquake, indicating shortening. This is confirmation that the PYRA station moved towards the south and the Indian Plate towards the north.

Integral analyses of the coordinate variations occurred during the earthquake

In order to ascertain the global movement of the Earth's crust during the earthquake and to study the oscillations of the points of the Pyramid Laboratory, an integral function of the data (PIF) was defined for each component (north, east and elevation Z) and analysed separately. The results are presented in Figures 6 and 7 for the north component, showing a constant increase up to the moment of the strong shock of

Table 3. *Station positions on 30 April 2015*

	Latitude (°)	Longitude (°)	Elevation (m)	RMS-Lat. (m)	RMS-Lon. (m)	RMS-Elev. (m)
HYDE	17.4172614	78.5508732	441.688	0.00047	0.00042	0.00167
KIT3	39.1347674	66.8854486	622.486	0.00038	0.00042	0.00160
LCK3	26.9121796	80.9556361	64.176	0.00037	0.00037	0.00146
LCK4	26.9121429	80.9556170	64.191	0.00037	0.00037	0.00146
LHAZ	29.6573335	91.1040304	3624.603	0.00031	0.00036	0.00131
PYRA	27.9575382	86.8149576	5032.242	0.00050	0.00057	0.00231
PBRI	11.6377803	92.7121366	−22.516	0.00065	0.00060	0.00219
URUM	43.8079498	87.6006701	858.879	0.00038	0.00031	0.00118

RMS is calculated in metres on 24 h data.

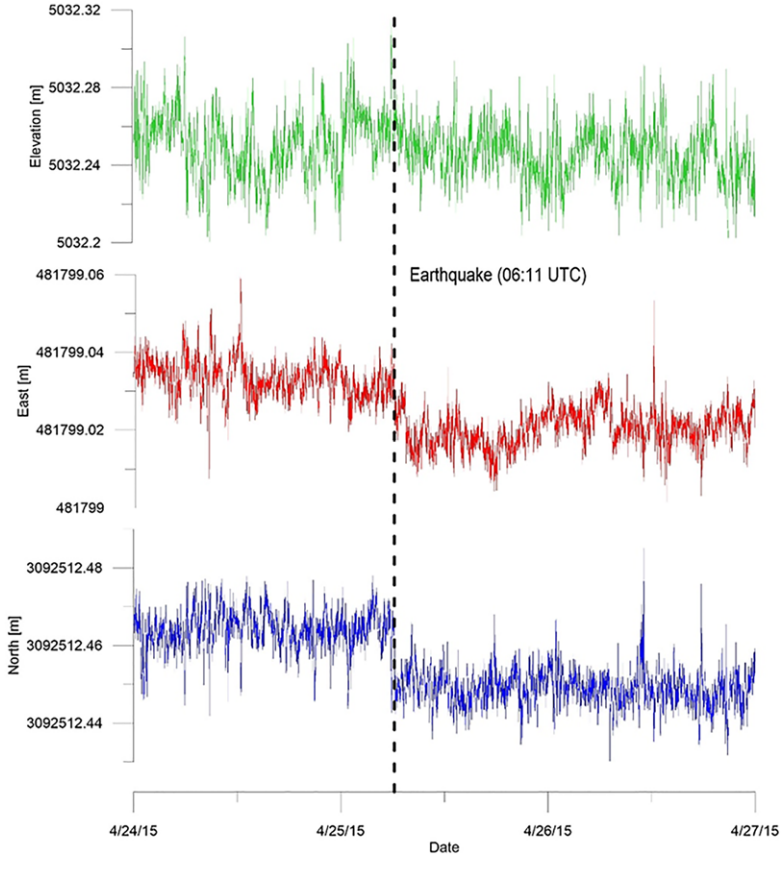

Fig. 6. Observed displacement at the PYRA station from 23 to 26 April 2015.

25 April at 06:11 UTC. After the shock, the function decreases constantly. The PIFs of the north and east components show an increasing trend pre-earthquake and a decreasing trend post-earthquake, with the maximum corresponding to the time of the main shock of the earthquake at 06:11 UTC. The behaviour of the height component is rather flat.

The earthquake of 12 May 2015

A similar analysis, as shown above, was performed on the data of 12 May 2015. Considering the plots of the available data, it seems that the behaviour of the north, east and elevation functions is very similar to that of the main shock of April 2015.

In Tables 6 and 7, the positions of the different IGS stations before (7 May 2015) and after the 12 May earthquake (15 May 2015) are shown; geographical coordinates WGS84 with their relative RMS are also shown. The method used to analyse these data is the same as in the previous cases.

The data show there was horizontal movement, with a period of 'assessment', followed by a normal trend, but with a centimetre difference in position. Elevational movement was either not present or was less than the measurement noise. Using UTM coordinates, it was possible to determine the movement derived from the earthquake (in metres) from 7 to 15 May 2015.

Table 4. *Co-seismic movements between 20 and 30 April 2015*

	Δ North (m)	Δ East (m)	Δ Elevation (m)
PYRA	−0.015	−0.017	−0.011

Co-seismic displacements: relative movements between PYRA and other IGS stations

One can determine the function of the positions of the Pyramid Lab and then calculate the PIF that

Table 5. *Distances of the IGS stations from the Pyramid Laboratory (April 2015)*

Station A	Station B	Distance (m) on 20 April 2015	Distance (m) on 30 April 2015	Δ (m)
PYRA	HYDE	1439865.430	1439865.401	−0.029
PYRA	KIT3	2209452.102	2209452.098	−0.004
PYRA	LCK3	590759.079	590759.059	−0.020
PYRA	LCK4	590761.819	590761.802	−0.016
PYRA	LHAZ	459293.658	459293.677	0.018
PYRA	PBRI	1902087.836	1902087.821	−0.014
PYRA	URUM	1755355.951	1755355.966	0.015

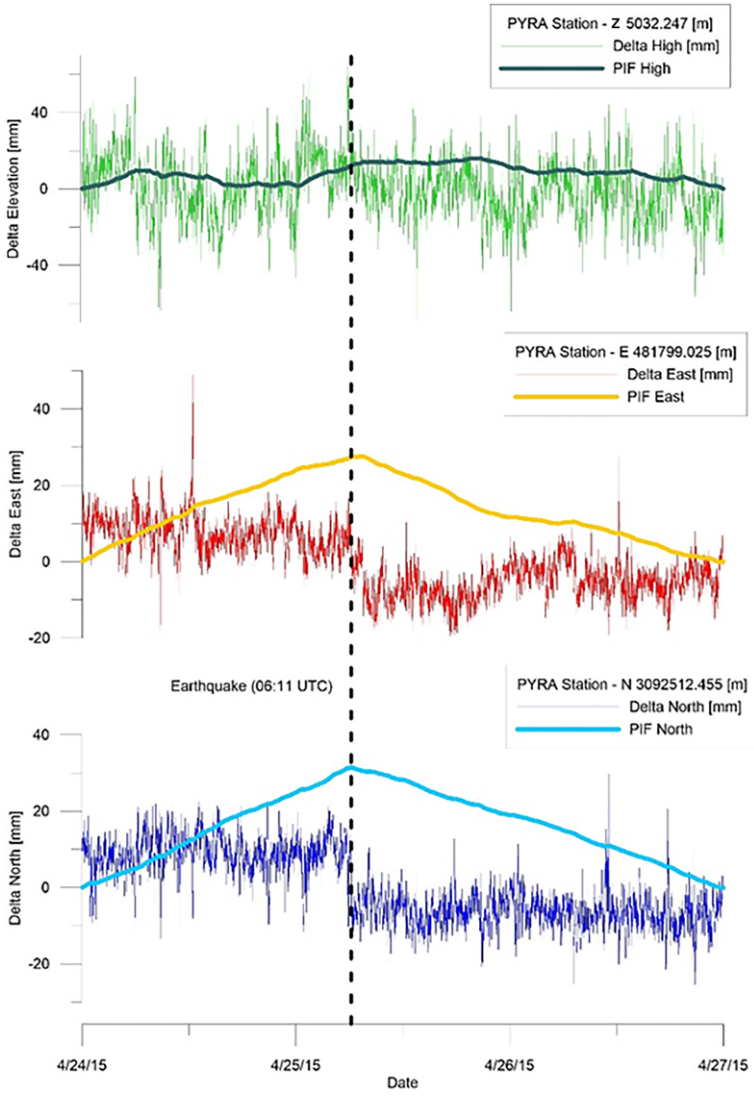

Fig. 7. Local and global (PIF) displacements at the PYRA station from 23 to 26 April 2015.

Table 6. *Station positions on 7 May 2015*

	Latitude (°)	Longitude (°)	Elevation (m)	RMS-Lat. (m)	RMS-Lon. (m)	RMS-Elev. (m)
HYDE	17.4172614	78.5508732	441.691	0.00048	0.00042	0.00172
KIT3	39.1347674	66.8854486	622.488	0.00040	0.00044	0.00173
LCK3	26.9121796	80.9556361	64.178	0.00039	0.00040	0.00155
LCK4	26.9121429	80.9556170	64.194	0.00039	0.00040	0.00155
LHAZ	29.6573335	91.1040304	3624.603	0.00033	0.00038	0.00140
PYRA	27.9575382	86.8149576	5032.242	0.00053	0.00060	0.00242
PBRI	11.6377802	92.7121366	−22.512	0.00069	0.00064	0.00238
URUM	43.8079498	87.6006701	858.874	0.00040	0.00033	0.00129

RMS is calculated in metres on 24 h data.

presents a behaviour very similar to the main shock of 25 April. Further, the height component 'Z' does not show a meaningful variation, while north and east increase up to the moment of the earthquake and decrease thereafter.

Integral analyses of the coordinate variations that occurred during the earthquake

In this case the direction of movement also shows a similar pattern as that observed during the occurrence of the main shock of the Gorkha earthquake. Computing the PIFs, a behaviour similar to that of the shock of 25 April 2015 is obtained. The increase of the north and east components is rather low, the maximum of the north component coincides with the time of the earthquake, while the east component reaches a maximum a few minutes later. Further, the elevation component shows no correlation with the time of the earthquake.

Discussion

With the processed results of the GNSS data recorded at the Pyramid Lab, we can investigate whether there was any permanent deformation of the Earth's crust during the earthquake and what was the extent of this deformation. It is also interesting to determine the net result after the earthquake. This can be detected by summing the movements of the Earth's crust during the tremors and following the return backwards after the earthquake. For this purpose, we have outlined a function P(t) providing the position of the GPS antenna sometime before, during and after the earthquake. The integral in time of this function PIF(t) provides the total movement of the point during the seismic activity:

$$\mathrm{PIF}(t) = \mathrm{PIF}(t-1) + P(t) \quad (1)$$

starting at the beginning of the observations (PIF(1) = 0) and calculated for all three components (Z, EW, NS) as can be seen in Figure 7. From the analysis of the PIFs, one can observe that the behaviour of the 'Z' component is rather flat, whereas, the EW component provides a maximum at the time of the earthquake. Similar attributes are also seen for the NS component, with lower intensity. It is also evident that the maximum for the NS component occurs two hours later during the earthquake of April, which may be due to the different distances of the GPS stations from the Pyramid Lab.

Table 7. *Station positions on 15 May 2015*

	Latitude (°)	Longitude (°)	Elevation (m)	RMS-Lat. (m)	RMS-Lon. (m)	RMS-Elev. (m)
HYDE	17.4172614	78.5508731	441.689	0.00049	0.00039	0.00152
KIT3	39.1347674	66.8854486	622.485	0.00042	0.00044	0.00182
LCK3	26.9121796	80.9556361	64.174	0.00042	0.00042	0.00182
LCK4	26.9121429	80.9556170	64.190	0.00042	0.00041	0.00163
LHAZ	29.6573335	91.1040304	3624.605	0.00036	0.00041	0.00163
PYRA	27.9575380	86.8149574	5032.244	0.00056	0.00065	0.00253
PBRI	11.6377803	92.7121366	−22.507	0.00067	0.00063	0.00235
URUM	43.8079498	87.6006701	858.875	0.00041	0.00033	0.00134

RMS is calculated in metres on 24 h data.

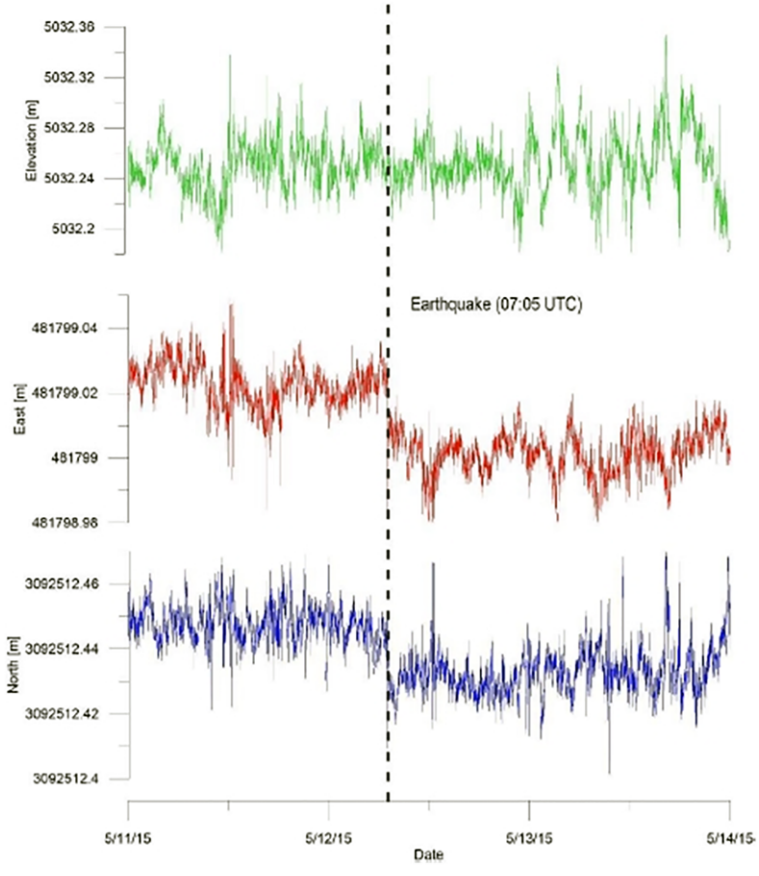

Fig. 8. Observed displacement at the PYRA station from 11 to 14 May 2015.

The displacement components of the IO-EVN broadband station, for the main shock and aftershock of 12 May (Fig. 5b, c) show a co-seismic offset of about 2–3, comparable with the offsets of the GPS station of Pyramid PYRA (Figs 6 & 8). In both cases the displacement movement of the vertical component during the earthquake (Figs 5b & 6) is downwards. On IO-EVN the NS component has an opposite co-seismic displacement for the main shock and the M_w 7.3 aftershock. On the EW component it is important to underline co-seismic displacement without permanent offset similar to that detected at the KTP station situated close to Kathmandu (Takai *et al.* 2016, fig. 5). However, for IO-EVN displacement, the first movement on the EW component for the main shock is towards the east, before the pulse of maximum amplitude, and the vertical component 'Z' does not show an apparent permanent deformation, as also reflected at the KTP station. It can also be seen that the IO-EVN displacement series needs a further detrending process for enhancing the signals.

Conclusions

The seismic movements of the earthquake, before and after the seismic event, can be detected and recorded by a GNSS station that can indicate not only the intensity of the tremors but also the size of the shifts for the point at the permanent GNSS station located close to the Gorkha Nepal earthquake. The present research demonstrates the importance of the precise calculation of the GNSS station coordinate as well as determining the sum of the movements noted by the Bernese software through the PIF. The constant increase in the north and east components before the earthquake may suggest a sequential analysis for a possible warning if systematic processing of the data is carried out. In view of the constant increase in the north and east components of the PIFs, one can suggest that a slope inversion might occur later. The maxima of the PIF north component occurs exactly at the time of the earthquake, as shown by the broadband IO-EVN seismic station. It would be meaningful to perform the same

analyses on the data recorded at other GNSS stations when earthquakes occur close to a recording station.

Acknowledgements Thanks to the late Prof. Mucciarelli (1960–2016), director of the CRS seismological section of the OGS, for the funding granted for this work and with which we were able to participate in the 30th HKT workshop at Dhera Dum (India), 6–8 October 2015.

Funding GP is grateful to the EvK2CNR Committee and OGS for funding (award ID0EAIAE969).

References

Ader, T., Avouac, J.P. *et al.* 2012. Convergence rate across the Nepal Himalaya and interseismic coupling on the Main Himalayan Thrust: implications for seismic hazard. *Journal of Geophysical Research*, **117**, B04403, https://doi.org/10.1029/2011JB009071

Adhikari, L.B., Gautam, U.P. *et al.* 2015. The aftershock sequence of the 2015 April 25 Gorkha-Nepal earthquake. *Geophysical Journal International*, **203**, 2119–2124, https://doi.org/10.1093/gji/ggv412

Avouac, J.-P., Meng, L., Wei, S., Wangand, T. & Ampuero, J.-P. 2015. Lower edge of locked Main Himalayan Thrust unzipped by the 2015 Gorkha earthquake. *Nature and Geoscience*, **8**, 708–711, https://doi.org/10.1038/ngeo2518

Bendat, J.S. & Piersol, A.G. 2010. *Random Data: Analysis and Measurement Procedures*. 4th edn. John Wiley & Sons, New York.

Bilham, R., Larson, K. & Freymueller, J. 1997. GPS measurements of present-day convergence across the Nepal Himalaya. *Nature*, **386**, 61–63, https://doi.org/10.1038/386061a0

Dach, R., Hugentobler, U. & Fridez, P. 2007. Bernese GPS software version 5.0. Astronomical Institute, University of Bern.

Denolle, M.A., Fan, W. & Shearer, P.M. 2015. Dynamic of the 2015 M7.8 Nepal earthquake. *Geophysical Research Letters*, **42**, 7467–7475, https://doi.org/10.1002/2015GL065336

Galetzka, J., Melgar, D. *et al.* 2015. Slip pulse and resonance of the Kathmandu basin during the 2015 Gorkha earthquake, Nepal. *Science Sciencemag.org*, 4 September, **349**, 1091–1095.

Gibbons, S.J. & Ringdal, F. 2006. The detection of low magnitude seismic events using array-based waveform correlation. *Geophysical Journal International*, **165**, 149–166, https://doi.org/10.1111/j.1365-246X.2006.02865.x

Grandin, R., Vallèe, M., Satriano, C., Lacassin, R., Klinger, Y., Simoes, M. & Bollinger, L. 2015. Rupture process of the Mw=7.9 2015 Gorkha earthquake (Nepal): insights into Himalayan megathrust segmentation. *Geophysical Research Letters,* **42** , 6229–6235, https://doi.org/10.1002/2015GL066044

Huang, H., Meng, L., Plasencia, M., Wang, Y., Wang, L. & Xu, M. 2016. Matched-filter detection of the missing pre-mainshock events and aftershocks in the 2015 Gorkha, Nepal earthquake sequence. *Tectonophysics*, **714**, 71–81, https://doi.org/10.1016/j.tecto.2016.08.018

Jouanne, F. 2015. The 25 April Gorkha earthquake Pre-, co- and post-deformations From GPS measurement. *Proceedings of the 30th Himalaya–Karakorum–Tibet Workshop – 2015*, WIHG, Dehradun, India, 6–8 October 2015, 108–110.

Pettenati, F., Cravos, C., Dawa Sherpa, T., Adhikari Sherpa, L., Plasencia Linares, M.P., Romanelli, M. & Verza, G. 2014. The installation of a new broadband seismometer to the EVK2-CNR Pyramid International Laboratory-Observatory (Everest, Nepal). *33° Convegno Nazionale Gruppo Nazionale di Geofisica della Terra Solida GNGTS*, Bologna, 25–27 November 2014.

Poretti, G., Calligaris, C., Tariq, S., Khan, H. & Zubair, F. 2010. The Nanga Parbat–Haramosh Monitoring Network. *29° Convegno GNGTS, Trieste*, 26–28 October 2010, 172, 173.

Poretti, G., Calligaris, C., Tariq, S. & Khan, H. 2011. Comparison between the Tectonic Movements of the Nanga Parbat-Haramosh Massif and Mt. Everest. *GNGTS Trieste*, 14–17 November 2011.

Poretti, G., Morsut, F. & Pettenati, F. 2015. Nepal earthquake evidence from GNSS data recorded at the Everest Pyramid Lab. *Proceedings of the 30th Himalaya–Karakorum–Tibet Workshop – 2015* (Abstract book), WIHG, Dehradun, India, 6–8 October 2015, 117–119.

Takai, N., Shigefuji, M., Rajaure, S., Bijukchhen, S., Ichiyanagi, M., Dhital, M.R. & Sasatani, T. 2016. Strong ground motion in the Kathmandu Valley during the 2015 Gorkha, Nepal, Earthquake. *Earth Planets and Space*, **68**, 10, https://doi.org/10.1186/s40623-016-0383-7